nature chemistry

ARTICLES

PUBLISHED ONLINE: 7 APRIL 2013 | DOI: 10.1038/NCHEM.1617

Catalytic control over supramolecular gel formation

Job Boekhoven, Jos M. Poolman, Chandan Maity, Feng Li, Lars van der Mee, Christophe B. Minkenberg, Eduardo Mendes, Jan H. van Esch* and Rienk Eelkema*

Low-molecular-weight gels show great potential for application in fields ranging from the petrochemical industry to healthcare and tissue engineering. These supramolecular gels are often metastable materials, which implies that their properties are, at least partially, kinetically controlled. Here we show how the mechanical properties and structure of these materials can be controlled directly by catalytic action. We show how *in situ* catalysis of the formation of gelator molecules can be used to accelerate the formation of supramolecular hydrogels, which drastically enhances their resulting mechanical properties. Using acid or nucleophilic aniline catalysis, it is possible to make supramolecular hydrogels with tunable gel-strength in a matter of minutes, under ambient conditions, starting from simple soluble building blocks. By changing the rate of formation of the gelator molecules using a catalyst, the overall rate of gelation and the resulting gel morphology are affected, which provides access to metastable gel states with improved mechanical strength and appearance despite an identical gelator composition.

Catalytic control over the formation of supramolecular structures is widespread in nature, directing vital processes such as cell motility, intracellular transport and muscle contraction, and resulting in the rapid turnover of self-assembled structures by acting on feedback-controlled processes[1]. In recent years, self-assembly of synthetic systems has seen major advances, particularly directed at the formation of dynamic and non-equilibrium structures[2–4]. However, in these artificial systems only a few specific examples of catalytic control over self-assembly exist in (auto)catalytic amphiphile formation and assembly[5–7], and in enzyme controlled peptide and surfactant assembly[8–17]. Vice versa, enzymatic catalysis of the disassembly of peptide-based gelators and dendrimer-based amphiphilic nanocontainers has been described[18,19]. Because material properties often depend on the rate of building-block assembly, they can potentially be controlled using chemical catalysis, thereby providing access to alternative self-assembly pathways and kinetically controlled non-equilibrium states. Moreover, catalysis of the formation of organic architectures offers the possibility to control the spatial and temporal distribution of soft materials and their associated properties. As such, catalytically controlled soft materials may find application in self-healing materials[20], for controlled-release purposes[21] and as actuators[22].

Here, we show how to control the rate of formation of supramolecular gels, and how this affects their material properties, by exploiting the susceptibility of formation of the gel monomers to catalytic action. Central to this concept are building blocks capable of self-assembling into fibrous structures, which form only on construction from smaller non-assembling fragments through the formation of a covalent bond. Catalytic action on the formation of this covalent bond can control the rate of assembly formation, which ultimately affects the morphology of the resulting materials and thus provides access to non-equilibrium metastable self-assembled materials.

The formation of molecular gels generally occurs through the self-assembly of low molecular weight (LMW) gelator molecules into elongated fibrous structures, which in turn form an entangled network in their solvent[23,24]. In such gels, the rate of formation of the fibres has a pronounced effect on fibre morphology and hence their macroscopic properties, but typically it is controlled via supersaturation levels, cooling rates and triggers such as light and pH[25–27]. Only very recently was it shown that the rate of enzyme-catalysed LMW gelator formation affects gel morphology[9]. Designing and applying LMW gelators that are capable of forming from non-gelating precursors through the creation of a covalent bond will enable us to investigate the influence of catalysis on self-assembly and material properties. In the past, *in situ* formation of supramolecular gelators has been reported, typically using two-component systems that form the gelating monomer either by covalent[28,29] or non-covalent[30,31] interactions. Remarkably, despite the prospects, so far the influence of catalysis on the formation and properties of these supramolecular materials has not been explored.

Results and discussion

The current study required a catalysis-responsive gelator, which was designed analogously to a highly efficient modular class of LMW hydrogelators based on a tris-functionalized cyclohexane scaffold[32], further developed in our labs in recent years[33]. In the current design, the three original hydrogen-bonding amide linkages are replaced by hydrazone links (**3** in Fig. 1). Low and high molecular weight gels that contain hydrazone bonds have been reported, which underlines the compatibility of the hydrazone bond with the aggregation process[34–36].

Structurally similar to amides, hydrazones are good hydrogen-bond acceptors and donors, and thereby provide the non-covalent interactions necessary for self-assembly. Hydrazone gelator **3** consists of a hydrophobic alkane core and three hydrogen-bonding hydrazone groups flanked by hydrophobic phenyl substituents. The phenyl moieties are decorated with oligoethylene glycol tails, which enhance the solubility of the building blocks (**2**) and prevent crystallization of the gelator (Fig. 1). Crucially, the gelator can be formed *in situ* by the reaction of the cyclohexane trishydrazide building block **1** and three molecules of aldehyde **2**. The rate of formation of the hydrazone bond, a prototypical reversible bond between a hydrazide and an aldehyde extensively applied in dynamic covalent chemistry[37,38], can be increased through both acid and nucleophilic aniline catalysis[39,40].

Department of Chemical Engineering, Delft University of Technology, Julianalaan 136, 2628 BL Delft, The Netherlands. *e-mail: j.h.vanesch@tudelft.nl; r.eelkema@tudelft.nl

© 2013 Macmillan Publishers Limited. All rights reserved.

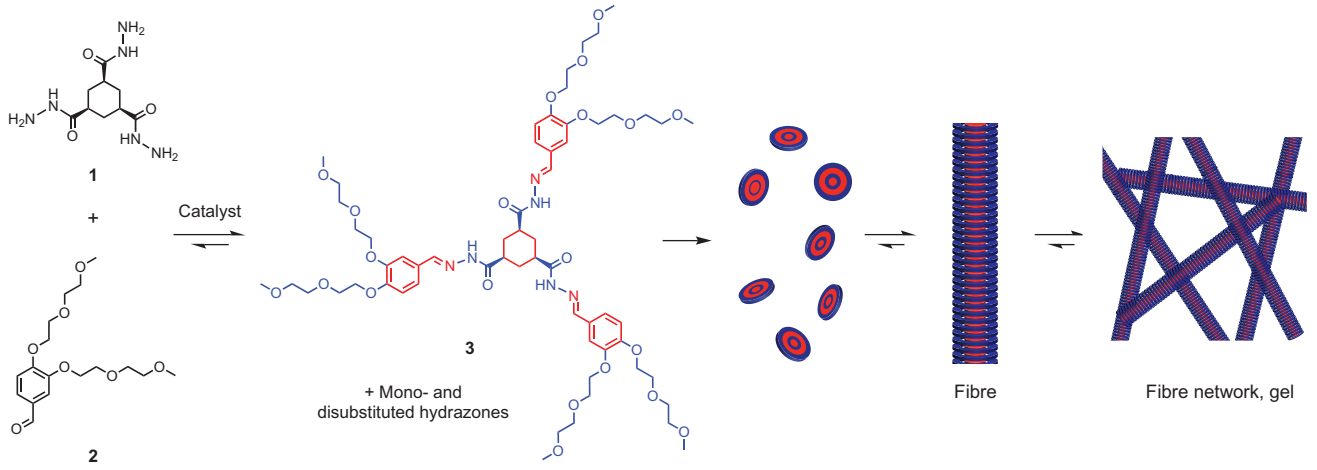

Figure 1 | Concept of a catalysed gelator and gel formation. Catalytic formation of trishydrazone hydrogelator **3** from soluble building blocks **1** and **2** leads to supersaturation followed by fibre formation, which eventually crosslink to form a network that traps the surrounding solvent, leading to gelation. Blue = hydrophilic, red = hydrophobic functional groups.

Mixing clear aqueous solutions of trishydrazide **1** and aldehyde **2** in a 1:6 molar ratio at pH 7.0 (1:2 ratio of hydrazide to aldehyde functional groups, [**1**] = 8 mM, 0.1 M phosphate buffer) at room temperature resulted in the formation of turbid solutions. Interestingly, at pH 5.0, mixing these solutions resulted in the formation of stable opalescent gels, with a critical gelation concentration (CGC) of 4.5 ± 0.5 mM (expressed in the starting concentration of **1**). Similarly, the same mixture at pH 7.0 in the presence of 10 mM aniline afforded a stable turbid gel with a CGC of 3.8 ± 0.5 mM (Fig. 2). Increasing the concentration of starting material **1** to 20 mM at pH 7.0 without catalyst did eventually result in the formation of weak crystalline gels, which indicated a significantly higher CGC in the absence of catalysts. High-performance liquid chromatography (HPLC) experiments showed, in all cases, the formation of >95% of the trishydrazone **3** and <5% of the bishydrazone, whereas no monohydrazone was observed. Gel formation could be reversed by applying strong acid (pH <1, gel → sol) and reinstated using base (pH >4, sol → gel), but the gels were stable to temperature increase (up to 120 °C), possibly as a result of a lower critical solution temperature of the oligoethylene glycol side chains. Clear differences were visible in the development of sample turbidity over time between catalysed and uncatalysed samples when studied by ultraviolet–visible spectroscopy (Fig. 2). The final turbidity (measured as the absorbance of 500 nm light) was highest for the uncatalysed sample and lowest for the acid-catalysed sample. Moreover, the rate of turbidity increase was drastically higher in the catalysed samples, with the highest rate observed for the acid-catalysed sample, reaching a maximum absorbance within 60 minutes. A somewhat lower but comparable rate was observed for the aniline-catalysed sample, whereas the uncatalysed sample took roughly nine hours to reach its final absorbance level. These results suggest a strong relationship between the rate of turbidity increase, and therefore of structure formation, and the morphology of the resulting material.

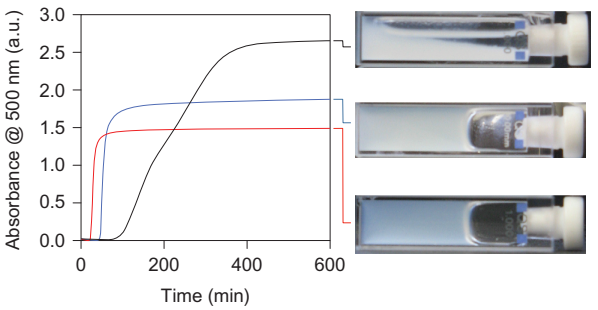

Figure 2 | Influence of catalysis on material formation and appearance. Turbidity measurements show the time-dependent absorbance of 500 nm light as a measure of structure formation (red line, pH 5.0; blue line, 10 mM aniline at pH 7.0; black line, pH 7.0 (**1**:**2** = 1:6, [**1**] = 8 mM; 0.1 M phosphate buffer)). The two catalysed samples (red and blue lines) show structure formation on significantly shorter time scales than the uncatalysed sample (black line). The resulting materials are shown on the right: the acid-catalysed gel (bottom) is more transparent than the aniline-catalysed gel (middle). The uncatalysed mixture cannot support the solvent and shows precipitation (top). a.u. = arbitrary units.

Indeed, both confocal laser scanning fluorescence microscopy and scanning electron microscopy showed the formation of dense homogeneous networks that consisted of heavily branched interconnecting fibres in both catalysed scenarios, whereas the uncatalysed system was made up of single poorly connected unbranched bundles of fibres and networks of thick fibre bundles (Fig. 3). Despite the differences in network morphology, cryotransmission electron microscopy showed that in all systems the gel networks consist of fibres up to 1 μm in length and 5.5 ± 1 nm thick, which in the uncatalysed case sometimes appeared to assemble into slightly thicker bundles (Supplementary Fig. S2). Wide-angle X-ray powder diffraction patterns of catalysed and uncatalysed gels showed main reflections at 27.0 and 4.1 Å, which are probably associated with the intercolumn distance and the intermolecular stacking distance within the columns, respectively, when compared to related single-crystal X-ray structures (Supplementary Fig. S4)[33]. No significant differences were observed between catalysed and uncatalysed samples, which indicates equivalent molecular organization in all cases.

The influence of catalysis on the material properties was studied by rheology, at [**1**] = 20 mM to ensure the formation of gels in all mixtures. Again, distinct differences between catalysed and uncatalysed samples were observed. Lowering the pH resulted in a drastic reduction of the gelation time, changing from 275 minutes at pH 7 to less than eight minutes at pH 5 (Fig. 4a). Addition of aniline to a pH 7 mixture had a similar effect, reducing the gelation time to less than 12 minutes with 50 mM aniline (Fig. 4b). Moreover, the catalysis greatly influenced the mechanical properties of the gels. Acid catalysis resulted in an increase of the maximum obtained storage modulus (G') by an order of magnitude to 50 kPa at pH 5

© 2013 Macmillan Publishers Limited. All rights reserved.

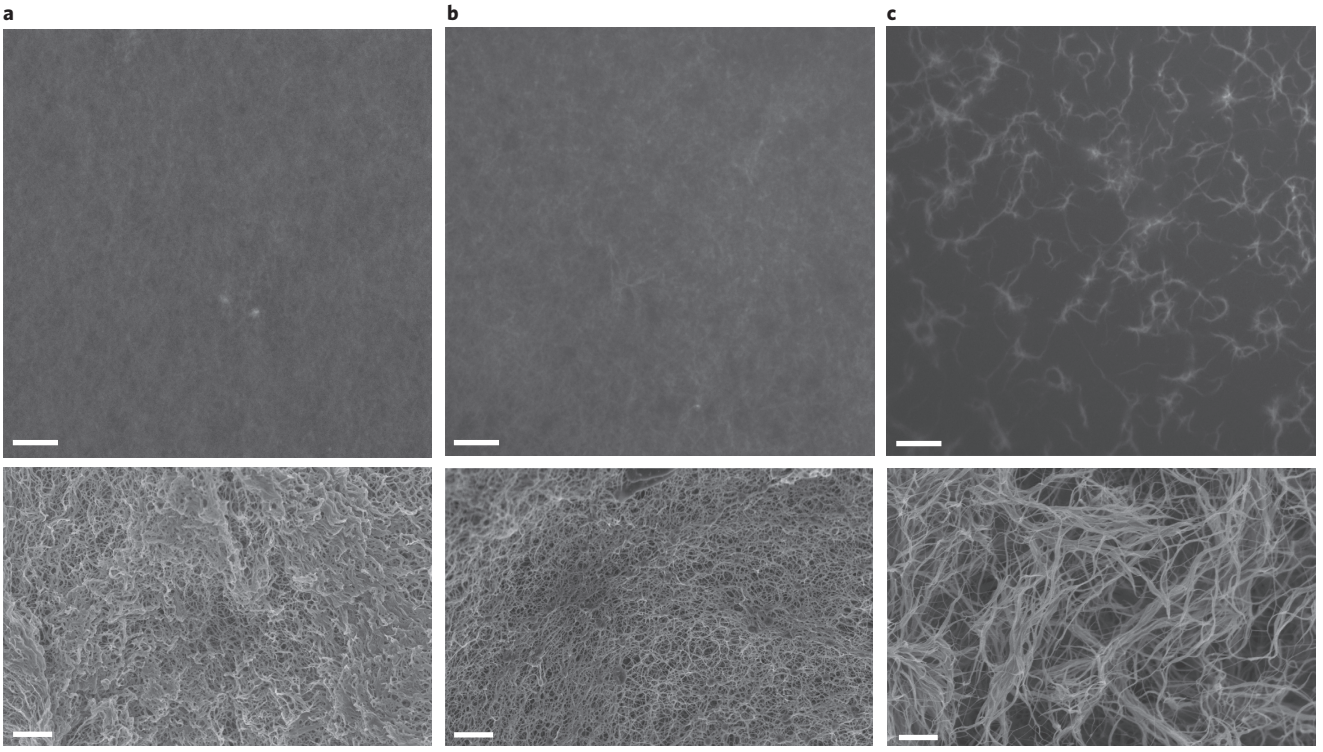

Figure 3 | Influence of catalysis on material morphology. a–c, Confocal laser scanning fluorescence micrographs (top) and scanning electron micrographs (bottom) show differences in network morphology and fibre thickness that depend on catalyst loading at pH 5.0 (**a**) and pH 7.0 with 10 mM aniline (**b**), and uncatalysed at pH 7.0 (**c**). Both catalysed samples (**a**,**b**) show thin highly branched fibres forming a dense network. In the uncatalysed scenario (**c**) thick less-branched fibres form a poorly connected network. All samples were prepared by mixing solutions of **1** and **2** ([**1**] = 4 mM, **1**:**2** = 1:6, 0.1 M phosphate buffer) and a 30 μM fluorescent probe at room temperature. Scale bars = 10 μm (top) and 500 nm (bottom).

(Fig. 4c). In the case of aniline catalysis, the maximum obtained storage modulus showed a maximum using 10 mM aniline catalyst, again leading to an increase in storage modulus by an order of magnitude (55 kPa, Fig. 4d). However, it was observed that higher aniline concentrations led to a decrease in storage modulus. Although high aniline concentrations did not lead to unexpected rate changes, changes in conversion, network morphology or CGC, we did observe the persistent formation of the amphiphilic aniline-derived imine of aldehyde **2** at high aniline concentrations (Supplementary Information), which may have a detrimental effect on the mechanical properties. Gel formation as observed by time-dependent rheology showed a two-stage process in both uncatalysed and catalysed scenarios, although less pronounced for the uncatalysed gel (Fig. 4e–g). In all cases the onset of percolation (when G' surpasses G'') was observed at an early stage in the process. HPLC analysis of the kinetics of formation of gelator **3** (Supplementary Fig. S6) showed that the majority of **3** was formed after reaching the onset of percolation, and revealed a clear relation between hydrazone formation (and thus catalytic action) and the evolution of the mechanical gel strength over time. A first plateau observed in the rheology curves (Fig. 4e–g) is probably associated with the addition of gelator molecules to the existing network formed at an early stage, causing it to stiffen or crosslink. At longer times, when the rate of formation of **3** increases, a further increase of the storage modulus (G') was observed until a second plateau was reached. This effect, much more pronounced in the catalysed samples, may be caused by the formation of new branched fibres interspersing with the existing network.

Additives to the gelation medium, such as ions or co-solvent, can have a profound effect on gel strength and appearance. To rule out the catalysts acting as mere solvent additives that change the quality of the gelation medium, CGCs were determined for gels prepared by dissolving separately synthesized catalyst-free **3** in the appropriate catalyst-containing media (pH 5, 10 mM aniline pH 7 and pH 7), followed by controlled and relatively fast gelation (Supplementary Information). In all cases CGCs of 4.5 ± 0.5 mM were recorded, indicative of a negligible influence of the catalyst on the properties of the medium at these catalyst concentrations, thereby pointing towards a relationship between the rate of gelator formation and the gel properties.

The observation that the stronger gels, obtained under catalytic conditions, contain a dense, heavily branched fibre network whereas the weaker uncatalysed mixtures are made up of unbranched fibre bundles (Fig. 3) suggests that the rate of gelator formation can influence the structure of the assembled materials. Analysis of the development of turbidity over time (Fig. 2), in terms of the dimensionality of structure formation using the Avrami equation[41], showed a significant difference in the Avrami coefficient n between the uncatalysed and catalysed samples, with $n = 1.4 \pm 0.2$ (pH 7), $n = 2.3 \pm 0.2$ (pH 5) and $n = 2.4 \pm 0.2$ (10 mM aniline) (Supplementary Fig. S10). These results confirm a fractal-like growth in the catalysed samples, which leads to a well-connected continuous network[42]. The lower dimensionality of the growth of the uncatalysed sample indicates the formation of fibrous structures with a lower degree of branching and thereby fewer interfibre connections, which is probably responsible for the significantly lower mechanical strength of the gels. It is therefore plausible that the increase in the rate of gelator formation caused by catalysis results in faster fibre growth, which causes the incorporation of local fibre defects during assembly and hence in branching of the fibre structures, and thus leads to fortification of the resulting network structure. These results show behaviour opposite to that of previously reported enzyme-catalysed fibre growth[9]. Those reports showed bundling and ordering of fibres that increased with

© 2013 Macmillan Publishers Limited. All rights reserved.

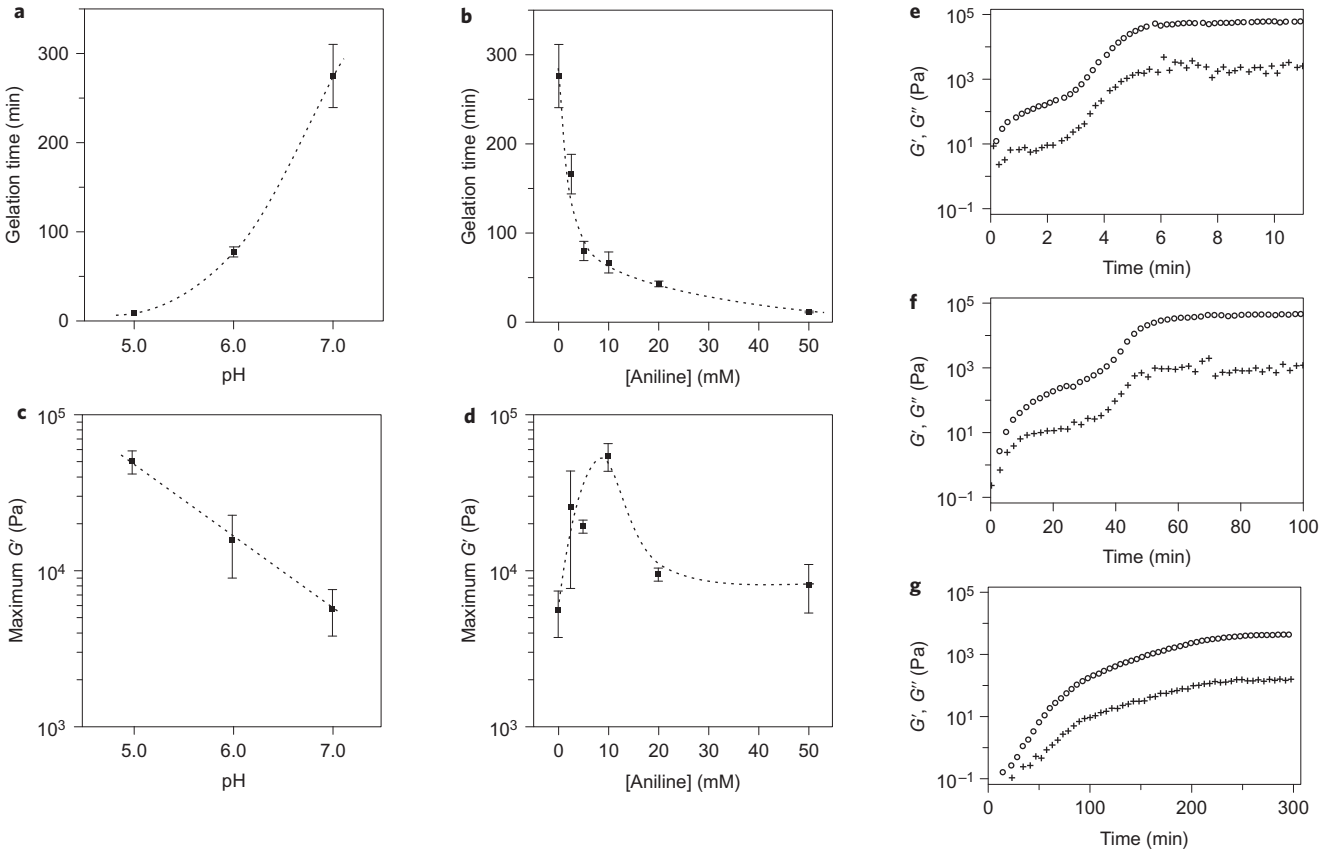

Figure 4 | Gel properties and formation dynamics depend on catalyst loading. a–d, Gel formation measured by rheology: the dependence on catalyst concentration of gelation time (**a**,**b**) and the maximum storage modulus (G') (**c**,**d**). Errors are the standard deviation from duplicate experiments; the lines are to guide the eye. Both gelation time and maximum storage modulus show a strong dependence on the amount of added catalyst: in the acid-catalysed scenario (**a**,**c**) the gelation time is reduced and the storage modulus increased with increasing catalyst concentration. The aniline-catalysed samples (**b**,**d**) show a more complex behaviour: although gelation time is reduced with increasing aniline concentration, the maximum storage modulus, after an initial increase, decreases again at very high aniline concentrations, most probably because of the formation of a surface-active adduct of aniline to **2**. **e–g**, The evolution of G' and G'' over time at pH 5.0 (**e**), pH 7.0 with 10 mM aniline (**f**) and pH 7.0 (**g**). All samples: **1**:**2** = 1:6, [**1**] = 20 mM; 0.1 M phosphate buffer.

increased catalyst concentration and an associated decreased catalyst mobility, whereas in the present system highly mobile, homogeneously dispersed catalysts (acid, aniline) control fibre branching, which leads to efficient crosslinking. As these gels all have identical gelator composition, the observed differences in mechanical properties and network morphologies are manifestations of various metastable thermodynamic states of the same self-assembled system, which can be addressed by changing the rates of gelator formation using catalysis.

Conclusions

We show here how both the rate of gel formation and the resulting mechanical properties can be controlled through *in situ* catalysis of the formation of gelator molecules. Drastic enhancements of rates of formation and mechanical strength of supramolecular hydrogels were observed using either acid or nucleophilic aniline catalysis. Analysis of the kinetic data points towards a mechanism in which a higher rate of gelator formation leads to an increased formation of defects in the gel fibre, thereby resulting in branching of the fibres, which subsequently strengthens the resulting gel. As such, catalytic control over building-block formation provides access to alternative kinetically stable non-equilibrium self-assembled materials. In the present system, catalysis enables the rapid formation of hydrogels from simple water-soluble building blocks under ambient conditions. In particular, aniline catalysis allows the formation of tunable hydrogels at physiological pH. In the future, catalysis could provide dynamic and spatial control of material formation and properties using, for instance, switchable catalysts[43–45] or catalytically active patterned surfaces.

Methods

Synthetic procedures. All compounds were synthesized from commercially available materials and characterized by ^{1}H and ^{13}C NMR spectroscopy, mass spectroscopy and infrared spectroscopy. See the Supplementary Information for the exact synthetic procedures.

General sample preparation. All solutions were prepared from aqueous 100 mM sodium phosphate buffer at the appropriate pH. Typical stock solutions of 40 mM hydrazide **1** and 240 mM aldehyde **2** where used. Most experiments were performed at an initial ratio of **1**:**2** = 1:6, that is two aldehyde groups per hydrazide group. Increasing or decreasing this ratio (either to 3:1 aldehyde:hydrazide or to 1:1 aldehyde:hydrazide) had no significant effect on the final product distribution. It did affect the overall kinetics of conversion, showing faster reactions at higher ratios.

CGC test procedure. A sample vial (2 ml) was filled with the appropriate volumes of stock solution and made up to 1 ml total volume by the addition of buffer. The vial was closed, shaken vigorously and allowed to stand overnight. The test tube was inverted to see whether a self-supporting gel had formed. The CGC is the point between the last concentration at which a gel is formed and the concentration at which the solvent can no longer be supported.

HPLC. The composition of gelator mixtures was analysed by HPLC, using a water:MeOH + 0.5% triethylamine gradient (Supplementary Fig. S5). Hydrazone formation and exchange was quenched by adding a 50 μl aliquot of reaction mixture to a mixture of 200 μl tetrahydrofuran + 200 μl water (saturated with triethylamine).

Confocal laser scanning microscopy. Confocal laser scanning micrographs were obtained in the fluorescence mode on a Zeiss LSM 700. To a stock solution of hydrazide **1** (at pH 5, pH 7 or with 10 mM aniline at pH 7) was added a fluorescein-derived aldehyde solution (see Supplementary Information) so that the final

© 2013 Macmillan Publishers Limited. All rights reserved.

concentration of the fluorescent probe was 30 μM. To form gels, 0.5 ml of this fluorescently labelled hydrazide solution was added to 0.5 ml aldehyde **2** solution. The mixture was immediately deposited into a polydimethylsiloxane cuvette closed off with a glass cover slide and was allowed to stand overnight. The laser beam was focused on a 40× oil immersion objective and the sensitivity of detectors and filters were adjusted accordingly to obtain the maximum signal to noise ratio.

Rheology. Oscillatory experiments were performed using a rheometer (AR G2, TA instruments) in a strain-controlled mode and equipped with a steel plate-and-plate geometry of diameter 40 mm equipped with a water trap. The temperature of the plates was controlled at 25±0.2 °C. All solutions were prepared in a vial after which the gel was poured directly onto the plate. See the Supplementary Information for the exact sample preparation.

Received 25 July 2012; accepted 27 February 2013; published online 7 April 2013

References

1. Stryer, L. *Biochemistry* (W. H. Freeman, 1995).
2. Carnall, J. M. A. *et al.* Mechanosensitive self-replication driven by self-organization. *Science* **327,** 1502–1506 (2010).
3. Capito, R. M., Azevedo, H. S., Velichko, Y. S., Mata, A. & Stupp, S. I. Self-assembly of large and small molecules into hierarchically ordered sacs and membranes. *Science* **319,** 1812–1816 (2008).
4. Korevaar, P. A. *et al.* Pathway complexity in supramolecular polymerization. *Nature* **481,** 492–496 (2012).
5. Kurihara, K. *et al.* Self-reproduction of supramolecular giant vesicles combined with the amplification of encapsulated DNA. *Nature Chem.* **3,** 775–781 (2011).
6. Bachmann, P. A., Luisi, P. L. & Lang, J. Autocatalytic self-replicating micelles as models for prebiotic structures. *Nature* **357,** 57–59 (1992).
7. Budin, I. & Devaraj, N. K. Membrane assembly driven by a biomimetic coupling reaction. *J. Am. Chem. Soc.* **134,** 751–753 (2012).
8. Williams, R. J. *et al.* Enzyme-assisted self-assembly under thermodynamic control. *Nature Nanotech.* **4,** 19–24 (2009).
9. Hirst, A. R. *et al.* Biocatalytic induction of supramolecular order. *Nature Chem.* **2,** 1089–1094 (2010).
10. Zhao, F. *et al.* β-Galactosidase-instructed formation of molecular nanofibers and a hydrogel. *Nanoscale* **3,** 2859–2861 (2011).
11. Gao, Y. *et al.* Enzyme-instructed self-assembly of peptide derivatives to form nanofibers and hydrogels. *Biopolymers* **94,** 19–31 (2010).
12. Webber, M. J., Newcomb, C. J., Bitton, R. & Stupp, S. I. Switching of self-assembly in a peptide nanostructure with a specific enzyme. *Soft Matter* **7,** 9665–9672 (2011).
13. Kühnle H. & Börner, H. G. Biotransformation on polymer–peptide conjugates: a versatile tool to trigger microstructure formation. *Angew. Chem. Int. Ed.* **48,** 6431–6434 (2009).
14. Xing, Y. Wang, C., Han, P., Wang, Z. & Zhang, X. Acetylcholinesterase responsive polymeric supra-amphiphiles for controlled self-assembly and disassembly. *Langmuir* **28,** 6032–6036 (2012).
15. John, G., Zhu, G., Li, J., & Dordick, J. S. Enzymatically derived sugar-containing self-assembled organogels with nanostructured morphologies. *Angew. Chem. Int. Ed.* **45,** 4772–4775 (2006).
16. Gao, J. *et al.* Enzyme promotes the hydrogelation from a hydrophobic small molecule. *J. Am. Chem. Soc.* **131,** 11286–11287 (2009).
17. Hahnab, M. E. & Gianneschi, N. C. Enzyme-directed assembly and manipulation of organic nanomaterials. *Chem. Commun.* **47,** 11814–11821 (2009).
18. van Bommel, K. J., Stuart, M. C. A., Feringa, B. L. & van Esch, J. Two-stage enzyme mediated drug release from LMWG hydrogels. *Org. Biomol. Chem.* **3,** 2917–2920 (2005).
19. Azagarsamy, M. A., Sokkalingam, P. & Thayumanavan, S. Enzyme-triggered disassembly of dendrimer-based amphiphilic nanocontainers. *J. Am. Chem. Soc.* **131,** 14184–14185 (2009).
20. Montarnal, D., Capelot, M., Tournilhac, F. & Leibler, L. Silica-like malleable materials from permanent organic networks. *Science* **334,** 965–968 (2011).
21. Boekhoven, J., Koot, M., Wezendonk, T. A., Eelkema, R. & van Esch, J. H. A self-assembled delivery platform with post-production tunable release rate. *J. Am. Chem. Soc.* **134,** 12908–12911 (2012).
22. He, X. *et al.* Synthetic homeostatic materials with chemo-mechano-chemical self-regulation. *Nature* **487,** 214–218 (2012).
23. Terech, P. & Weiss, R. G. Low molecular mass gelators of organic liquids and the properties of their gels. *Chem. Rev.* **97,** 3133–3160 (1997).
24. Steed, J. W. Supramolecular gel chemistry: developments over the last decade. *Chem. Commun.* **47,** 1379–1383 (2011).
25. Li, J. L., Liu, X. Y., Wang, R. Y. & Xiong, J. Y. Architecture of a biocompatible supramolecular material by supersaturation-driven fabrication of its fiber network. *J. Phys. Chem. B* **109,** 24231–24235 (2005).
26. de Jong, J. J. D., Lucas, L. N., Kellogg, R. M., van Esch, J. H. & Feringa, B. L. Reversible optical transcription of supramolecular chirality into molecular chirality. *Science* **304,** 278–281 (2004).
27. Chen, L. *et al.* Self-assembly mechanism for a naphthalene-dipeptide leading to hydrogelation. *Langmuir* **26,** 5232–5242 (2010).
28. Suzuki, M. *et al.* Effects of hydrogen bonding and van der Waals interactions on organogelation using designed low-molecular-weight gelators and gel formation at room temperature. *Langmuir* **19,** 8622–8624 (2003).
29. Boekhoven, J. *et al.* Dissipative self-assembly of a molecular gelator by using a chemical fuel. *Angew. Chem. Int. Ed.* **49,** 4825–4828 (2010).
30. Hunt, J. N. *et al.* Tunable, high modulus hydrogels driven by ionic coacervation. *Adv. Mater.* **23,** 2327–2331 (2011).
31. Hirst, A. R. *et al.* Low-molecular-weight gelators: elucidating the principles of gelation based on gelator solubility and a cooperative self-assembly model. *J. Am. Chem. Soc.* **130,** 9113–9121 (2008).
32. Hanabusa, K., Kawakami, A., Kimura, M. & Shirai, H. Small molecular gelling agents to harden organic liquids: trialkyl *cis*-1,3,5-cyclohexanetricarboxamides. *Chem. Lett.* 191–192 (1997).
33. van Bommel, K. J. *et al.* Responsive cyclohexane-based low-molecular-weight hydrogelators with modular architecture. *Angew. Chem. Int. Ed.* **43,** 1663–1667 (2004).
34. Sreenivasachary, N. & Lehn, J. M. Gelation-driven component selection in the generation of constitutional dynamic hydrogels based on guanine-quartet formation. *Proc. Natl Acad. Sci. USA* **102,** 5938–5943 (2005).
35. Deng, G., Tang, C., Li, F., Jiang, H. & Chen, Y. Covalent cross-linked polymer gels with reversible sol-gel transition and self-healing properties. *Macromolecules* **43,** 1191–1194 (2010).
36. Ossipov, D. A., Yang, X., Varghese, O., Kootala, S. & Hilborn, J. Modular approach to functional hyaluronic acid hydrogels using orthogonal chemical reactions. *Chem. Commun.* **46,** 8368–8370 (2010).
37. Corbett, P. T. *et al.* Dynamic combinatorial chemistry. *Chem. Rev.* **106,** 3652–3711 (2006).
38. Lehn, J. M. Dynamic combinatorial chemistry and virtual combinatorial libraries. *Chem. Eur. J.* **5,** 2455–2463 (1999).
39. Dirksen, A., Dirksen, S., Hackeng, T. M. & Dawson, P. E. Nucleophilic catalysis of hydrazone formation and transimination: implications for dynamic covalent chemistry. *J. Am. Chem. Soc.* **128,** 15602–15603 (2006).
40. Bhat, V. T. *et al.* Nucleophilic catalysis of acylhydrazone equilibration for protein-directed dynamic covalent chemistry. *Nature Chem.* **2,** 490–497 (2010).
41. Liu, X. Y. & Sawant, P. D. Formation kinetics of fractal nanofiber networks in organogels. *Appl. Phys. Lett.* **79,** 3518–3520 (2001).
42. Liu, X. Y. & Sawant, P. D. Mechanism of the formation of self-organized microstructures in soft functional materials. *Adv. Mater.* **14,** 421–426 (2002).
43. Gianneschi, N. C., Nguyen, S. T. & Mirkin, C. A. Signal amplification and detection via a supramolecular allosteric catalyst. *J. Am. Chem. Soc.* **127,** 1644–1645 (2005).
44. Peters, M. V., Stoll, R. S., Kuehn, A. & Hecht, S. Photoswitching of basicity. *Angew. Chem. Int. Ed.* **47,** 5968–5972 (2008).
45. Piermattei, A., Karthikeyan, S. & Sijbesma, R. P. Activating catalysts with mechanical force. *Nature Chem.* **1,** 133–137 (2009).

Acknowledgements

The authors acknowledge the European Commission (a Marie Curie European Reintegration grant, R.E.) and the Netherlands Organisation for Scientific Research (a VENI grant (R.E.), a VICI grant (J.H.v.E., J.B.) and an ECHO grant (R.E., J.H.v.E., J.M.P.)) for funding.

Author contributions

J.B., R.E. and J.H.v.E. designed the experiments, J.B., J.M.P., C.B.M., F.L., E.M. and R.E. performed the experiments and analysed the data, J.M.P., C.B.M., L.v.d.M., C.M. and R.E. synthesized the molecules, R.E. and J.H.v.E. guided the research and all authors contributed to discussing the results and editing the manuscript. R.E. wrote the manuscript.

Additional information

Supplementary information and chemical compound information are available in the online version of the paper. Reprints and permissions information is available online at www.nature.com/reprints. Correspondence and requests for materials should be addressed to J.H.v.E. and R.E.

Competing financial interests

The authors declare no competing financial interests.

© 2013 Macmillan Publishers Limited. All rights reserved.